[redacted]

NACA

RESEARCH MEMORANDUM

AN EXPERIMENTAL INVESTIGATION AT SUBSONIC AND SUPERSONIC SPEEDS OF THE TORSIONAL DAMPING CHARACTERISTICS OF A CONSTANT-CHORD CONTROL SURFACE OF AN ASPECT RATIO 2 TRIANGULAR WING

By David E. Reese, Jr.

Ames Aeronautical Laboratory
Moffett Field, Calif.

NATIONAL ADVISORY COMMITTEE
FOR AERONAUTICS

WASHINGTON

July 2, 1953

[redacted] RESEARCH

[redacted]

[redacted]

NATIONAL ADVISORY COMMITTEE FOR AERONAUTICS

RESEARCH MEMORANDUM

AN EXPERIMENTAL INVESTIGATION AT SUBSONIC AND SUPERSONIC SPEEDS OF THE TORSIONAL DAMPING CHARACTERISTICS OF A CONSTANT-CHORD CONTROL SURFACE OF AN ASPECT RATIO 2 TRIANGULAR WING

By David E. Reese, Jr.

SUMMARY

The results of a wind-tunnel investigation of the torsional damping characteristics of a constant-chord control surface are presented herein. The control surface was hinged at its leading edge and had an area equal to 23.7 percent of the exposed area of one wing panel of the aspect ratio 2 triangular wing. The test was conducted over a Mach number range of 0.6 to 0.9 and 1.3 to 1.9. The effects of variations in the control-surface oscillation amplitude, angle of attack, and frequency on the torsional damping coefficient were investigated. A cancellation technique was used to obtain the above data in forced-oscillation tests.

The test results showed the damping coefficient at supersonic speeds to be near zero with a tendency toward instability at low supersonic Mach numbers. The damping coefficients at subsonic speeds were stable throughout the Mach number range tested. The effects of variations in control-surface oscillation amplitude and angle of attack on the damping coefficient were small. Variations in frequency up to reduced frequencies of 0.030 had no apparent effect on the damping coefficient at supersonic speeds. At subsonic speeds, an increase in damping coefficient with increasing frequency was noted, but it was concluded that the presence of the wind-tunnel walls might have some effect on the data in this region.

Measurement of the aerodynamic restoring moments showed good agreement with static tests.

INTRODUCTION

As flight speeds have progressed into the transonic and supersonic regions, a need for information on the behavior of controls at these speeds has arisen. Recent studies have been made on the static loads occurring on control surfaces at high speeds but there is still a lack

of information in the field of dynamic loads. In particular, information is needed on the aerodynamic damping of control surfaces for flutter studies and servo-system design.

The present paper is concerned with a study that has been made to develop suitable equipment and techniques for obtaining control-surface damping derivatives from wind-tunnel tests. The technique and a description of the equipment that have evolved from this study are presented. This technique was applied to the determination of the nondimensional torsional damping-moment coefficient of an oscillating constant-chord control surface mounted on the trailing edge of a triangular wing of aspect ratio 2. The effects on this coefficient of the variation in control-surface oscillation amplitude, angle of attack, and frequency were measured over a Mach number range of 0.6 to 0.9 and 1.3 to 1.9.

SYMBOLS

C_h hinge-moment coefficient, $\frac{\text{hinge moment}}{\frac{1}{2}\rho V^2 Sc}$

$C_{h_{\dot{\delta}}}$ torsional damping-moment coefficient, $\frac{\partial C_h}{\partial(\dot{\delta}c/2V)}$

D damping parameter, ft-lb-sec

D.H. damping moment, ft-lb

H moment in-phase with δ, ft-lb

I control-surface moment of inertia, slug-ft^2

K spring constant, ft-lb/radian

M Mach number, $\frac{V}{\text{speed of sound}}$

S control surface area, sq ft

T tunnel stagnation temperature, $^\circ F$

V velocity of air, ft/sec

c control-surface chord, ft

f frequency of oscillation, cps

k reduced frequency, $\frac{\omega c}{2V}$

Δ	twist of strain-gage member ($\Delta = \delta_i - \delta$ and is proportional to strain-gage output)
α	angle of attack, deg
δ	control-surface deflection, deg
φ	phase angle, deg
ρ	mass density of air, slugs/cu ft
ω	angular frequency, $2\pi f$, radians/sec

Subscripts

a	aerodynamic
g	strain gage
h	hinge
i	input
o	maximum
t	total
w.o.	wind off

APPARATUS

Wind Tunnel

The model was tested in the Ames 6- by 6-foot supersonic wind tunnel which is of the closed-return, variable-density type and has a Mach number range of 0.6 to 0.9 and 1.2 to 1.9. A detailed description of the flow characteristics of this wind tunnel can be found in reference 1.

Model

The model used in this investigation consisted of a slender body of revolution in combination with an aspect ratio 2 triangular wing. The wing had NACA 0005 sections in streamwise planes. The dimensions of the wing-fuselage combination are given in figure 1. One wing panel of the

model was fitted with a constant-chord control surface with an area equal to 23.7 percent of the exposed area of the wing panel. It was hinged at its leading edge. A piano-type hinge was used originally but proved to have a friction damping several times the aerodynamic damping. The final hinge used was a modification of the original hinge made by removing all but three bushings, one at each end and one at the center of the hinge. A 1/16-inch-diameter steel hinge pin extended the length of the hinge with sufficient clearance in the bushings to insure minimum hinge friction. The model was constructed of steel with the exception of the control surface, which was fabricated from aluminum in order to keep its weight to a minimum. A photograph of the model is shown in figure 2.

A three-phase induction motor, used to oscillate the flap, was mounted in a cutout in the fuselage. The torque from this motor was transmitted to the control surface through a right-angle drive linkage. Photographs of the drive system are shown in figure 3. It was desired that the control surface be driven in sinusoidal oscillations. To achieve perfect sinusoidal motion would require the use of a scotch-yoke type of drive linkage. Since this system is difficult to fabricate on a small scale, the present system was chosen. Calculations showed that such a motion would deviate from a pure sine wave by only 0.13 percent at the maximum value of the displacement. A schematic drawing of the drive system is shown in figure 4.

Instrumentation

Two quantities were recorded during the investigation: instantaneous hinge moment and instantaneous position. A resistance-type strain gage mounted on the torsion member connecting the control surface to the drive system was used to measure the hinge moment of the control surface. A signal proportional to the position of the control system was produced by an acceleration-type indicating device. This device consisted of a cantilever beam mounted rigidly on that portion of the control surface which extended inside the fuselage cutout. A strain gage mounted on the beam produced a signal proportional to the acceleration of the beam mass. The natural frequency of the beam was 500 cycles per second or 10 times the maximum driving frequency of the flap. It can be shown that under these conditions, the acceleration of the beam is very nearly 180° out of phase with its position. Hence, with a change in sign, this signal could be used to indicate the position of the control surface. The two signals were recorded by a photographic oscillograph, using D'Arsonval galvanometer elements.

TEST METHODS

One of the major difficulties involved in obtaining out-of-phase (damping) moments in a forced-oscillation test is that the in-phase (stiffness and inertia) moments are usually much greater than the desired damping moments. Several methods have been used to overcome this difficulty (ref. 2). In order to illustrate how the method of this investigation was devised and used, an analysis of the mechanical system is given in the following paragraphs.

Theory of Test Method

A schematic diagram of the control-surface strain-gage combination is shown in the following sketch:

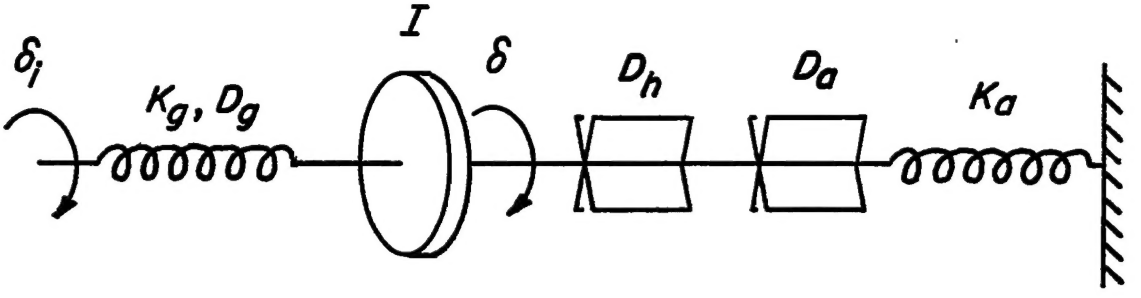

Sketch (a)

where

δ_i input angle - set by mechanical drive system, radians

K_g spring constant of the strain-gage member, ft-lb/radian

D_g internal damping of strain-gage member, ft-lb-sec

I moment of inertia of control surface, strain gage, and position indicator, slug-ft^2

δ deflection angle of the control surface, radians

D_h damping of hinge, ft-lb-sec

D_a aerodynamic damping, ft-lb-sec

K_a aerodynamic spring constant (restoring moment), ft-lb/radian

Writing the differential equation of motion for this system assuming positive angles and moments in the direction indicated

$$-I\ddot{\delta} - D_a\dot{\delta} - D_h\dot{\delta} - D_g(\dot{\delta}_i - \dot{\delta}) + K_g(\delta_i - \delta) - K_a\delta = 0 \qquad (1)$$

where

$$(\ddot{}) \equiv \frac{d^2}{dt^2}(\ ) \ , \ (\dot{}) \equiv \frac{d}{dt}(\ )$$

The input moment to the flap is represented by $K_g(\delta_i - \delta)$. This input is measured by the strain gage whose output is proportional to the deflection, $\delta_i - \delta$, of the strain-gage member. Substituting $\Delta = \delta_i - \delta$ into equation (1) and eliminating δ, results in:

$$I\ddot{\Delta} + (D_a + D_h - D_g)\dot{\Delta} + (K_a + K_g)\Delta = I\ddot{\delta}_i + (D_a + D_h)\dot{\delta}_i + K_a\delta_i \qquad (2)$$

The solution to the particular integral of the above differential equation in terms of a sinusoidal driving motion $\delta_i = \delta_{i_o}\sin\omega t$ is

$$\Delta = \Delta_o\sin(\omega t + \varphi)$$

where

$$\Delta_o = \delta_{i_o}\sqrt{\frac{(K_a - I\omega^2)^2 + (D_a + D_h)^2\omega^2}{(K_a + K_g - I\omega^2)^2 + (D_a + D_h - D_g)^2\omega^2}} \qquad (3)$$

and

$$\varphi = \tan^{-1}\frac{(D_a + D_h)\omega}{K_a - I\omega^2} - \tan^{-1}\frac{(D_a + D_h - D_g)\omega}{K_a + K_g - I\omega^2} \qquad (4)$$

In order to simplify these expressions, the relative magnitudes of the various terms must be examined. The following quantities were obtained from a stress analysis of the strain-gage member and wind-off tests:

$$K_g = 1060 \text{ ft-lb/radian}$$

$$I = 0.000276 \text{ slug-ft}^2$$

For a frequency of 50 cycles per second (maximum frequency for which data were obtained),

$$I\omega^2 = 27.2 \text{ ft-lb/radian}$$

In addition, experience has shown that the damping term $(D_a + D_h - D_g)\omega$ has a value less than 1.7 ft-lb per radian. Since both these terms are very small compared to $K_a + K_g$, equations (3) and (4) may be rewritten as

$$\Delta_o = \delta_{i_o} \frac{\sqrt{(K_a - I\omega^2)^2 + (D_a + D_h)^2\omega^2}}{K_a + K_g} \tag{5}$$

$$\varphi = \tan^{-1} \frac{(D_a + D_h)\omega}{K_a - I\omega^2} \tag{6}$$

Evaluation of Damping Moments

A vector diagram illustrating the moments involved in equations (5) and (6) is shown in the following sketch:

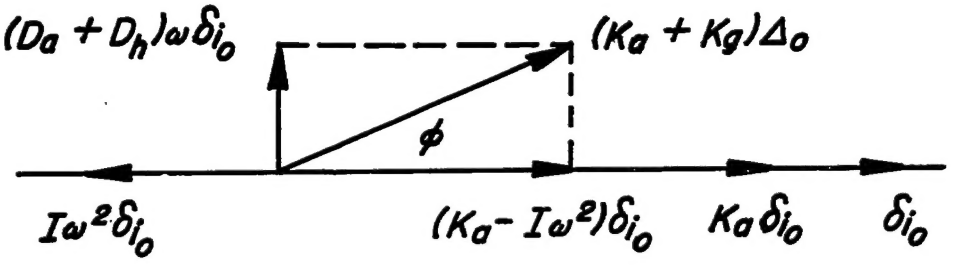

Sketch (b)

[redacted]

It can be seen that if $K_a = I\omega^2$, the resulting hinge moment is purely damping. This equality could be attained during the test by varying the tunnel pressure while holding the frequency fixed or by varying the frequency at a fixed tunnel pressure. Neither of these two alternatives was desirable in obtaining all the test data. The latter was used, however, to provide check points during the test. The same canceling effect can be accomplished by adding electrically a signal 180° out of phase with the signal proportional to $K_a - I\omega^2$. By adjustment of the magnitude of the added signal, the in-phase component, $K_a - I\omega^2$, can be canceled out and the total damping moment can be read directly.

For this investigation, the electrical signal used for cancellation purposes was produced by a slide-wire potentiometer. A potentiometer was chosen to produce the cancellation signal since it would produce a signal with a sufficiently small phase angle, relative to the motion of its wiper arm, to enable accurate cancellation of the in-phase component, provided the inductive and capacitive effects of the coil and wiper contact were small. It will be indicated shortly that these effects are small enough to be negligible for this investigation.

The potentiometer was mounted in the fuselage with the wiper arm attached to the linkage between the motor and the control surface. The output of the potentiometer was then directly proportional to the displacement of the control surface. To cancel the in-phase moments, the output of the potentiometer was connected to the output of the hinge-moment strain gage in such a manner as to oppose the existing in-phase signal. The magnitude of the canceling signal could be adjusted by changing the value of the voltage supplied to the potentiometer.

The point at which the in-phase signal was equal to the canceling signal was determined by changing the voltage to the potentiometer until the total-moment signal reached a minimum peak value. In this manner the vector $K_a - I\omega^2$ was canceled at all test points.

In order to check the accuracy of the electrical cancellation technique, the data obtained by this method were compared with the check points mentioned above. Since, as is shown later, frequency had no apparent effect on the damping coefficients at supersonic speeds, the fact that the data obtained with the canceling circuit agreed, within the uncertainty calculated in a subsequent section, with that obtained without the canceling circuit showed the effectiveness of the electrical cancellation technique.

Evaluation of In-Phase Moments

In a series of wind-tunnel tests to evaluate the magnitude of the in-phase aerodynamic moments, the cantilever-beam accelerometer mentioned

in the section on instrumentation was used to cancel the inertia moment of the control surface. Since the signal of the accelerometer was proportional to ω^2, the canceling circuit could be adjusted before the test to cancel the inertia moment and that setting would remain throughout the test. With reference to sketch (b), the inertia moment, $I\omega^2$, was canceled by the accelerometer signal leaving the vector sum of the restoring moment and the damping moment. Since the damping moment was less than 1 percent of the total aerodynamic moment, the value recorded was taken as the in-phase aerodynamic moment directly.

TESTS

The investigation of the torsional damping of the control surface was conducted over a Mach number range of 0.6 to 0.9 and 1.3 to 1.9. The Reynolds number for the entire test was 1.6×10^6 per foot. Data were obtained at 0° angle of attack at both subsonic and supersonic Mach numbers. Since the wind tunnel choked at angles of attack greater than 8° for the higher subsonic Mach numbers, data were obtained at $\alpha = 5^\circ$ for Mach numbers less than 1. For Mach numbers greater than 1, data were also obtained for $\alpha = 10^\circ$.

The maximum amplitude of the control-surface oscillations was set at 5°, 3°, and 1°, referred to the chord line of the wing. The flap was driven at two frequencies, 25 and 50 cycles per second, at each data point.

Tests were also made with boundary-layer transition fixed by means of a roughened area along the leading edge of the wing. It was felt that this type of test would be more valuable in the assessment of the importance of scale effect than the usual Reynolds number variation, since the range over which the Reynolds number could be varied was small enough to raise doubts about its having any significant effect on the boundary layer.

Reduction of Data

A typical record obtained during the wind-tunnel tests is shown in figure 5. The high harmonic content of the damping-moment trace is a result, for the most part, of the clearance between the hinge pin and the bushings that was necessary to give a low friction damping in the hinge. In addition, some aerodynamic disturbances were present due to the turbulence in the air stream. As a result of this harmonic content, a harmonic analysis was necessary to obtain the out-of-phase component of the fundamental frequency. Three consecutive cycles were analyzed

and an average of the three cosine components of the total moment at the fundamental frequency was taken as the damping moment.

The wind-off damping (hinge friction) was determined by driving the control surface in the wind tunnel at low pressure before and after each test. The average of the two values of damping moment obtained was used as the hinge damping moment for that test.

The aerodynamic damping moment was obtained by subtracting the wind-off damping from the total wind-on damping moment. This moment was reduced to coefficient form in the following manner:

$$C_h = \frac{-(D.H._t - D.H._{w.o.})}{\frac{1}{2}\rho V^2 Sc} \tag{7}$$

Writing the damping-moment coefficient in the form used in dynamic stability analyses,[1]

$$C_{h_{\dot{\delta}}} = \frac{\partial C_h}{\partial\left(\frac{\dot{\delta}c}{2V}\right)} = \frac{-4(D.H._t - D.H._{w.o.})}{\rho V S c^2 \omega \delta_{i_o}} \tag{8}$$

Hinge moments obtained from the in-phase tests were reduced to coefficient form as follows:

$$C_h = \frac{H}{\frac{1}{2}\rho V^2 Sc} \tag{9}$$

[1]Since the deflection of the strain-gage member, Δ, is very small relative to the control-surface deflection angle, δ, $\delta_i \approx \delta$. Hence,

$$\dot{\delta} \approx \dot{\delta}_i = \omega \delta_{i_o} \cos \omega t$$

Corrections to Data

No corrections were made to the hinge-moment coefficients obtained at subsonic speeds. The author knows of no published corrections for the effects of the tunnel walls on the oscillatory air forces of a subsonic three-dimensional wing. The considerations of Runyan and Watkins in reference 3 lead to a wind-tunnel resonant frequency for two-dimensional flow and this information has been used to compute the curves shown in figure 6. Inspection of these curves shows that the test frequencies, particularly at $M = 0.9$, are of the same order of magnitude as the tunnel resonant frequencies. In fact, at a Mach number of 0.90, the check poin at which the inertia moment canceled the in-phase aerodynamic moment occurred at the resonant frequency of the wind tunnel at that Mach number. These check points are shown in figures 8 and 9 as filled-in points. It is apparent from these figures that, at Mach numbers of 0.60 and 0.80, the check points are consistent with the frequency effects shown by the data obtained at 25 and 50 cycles per second; this is not true at a Mach number of 0.90, however. With the exception of the points taken at a flap oscillation amplitude of $\pm 1^{\circ}$, the data show a considerable drop in the value of the damping-moment coefficient at the check point. It is possible, therefore, that these data might be influenced by the effect of the the tunnel walls in a manner similar to that shown in reference 4.

The Mach number and dynamic pressure of the subsonic flow were corrected for blockage effects by the method presented in reference 5. At a Mach number of 0.9, these corrections amounted to an increase of 3 percent in the Mach number and dynamic pressure over the value obtained from measurement made without a model in the wind tunnel.

No corrections were made to either the flow conditions or the hinge-moment data at supersonic speeds.

Precision of Data

From equation (8), it can be seen that the precision of the data depends on the accuracy of measurement of four quantities: moment, density, velocity, and frequency. The measurement of the moment trace for use in the harmonic analyses was done on a type 38 telereader. This machine magnified the trace two and one-half times for ease of reading and had a least reading of 0.001 inch on the oscillograph record. However, inspection of the amplitudes of the wind-off damping moments showed an average variation from one cycle to another of ± 0.020 inch-pounds. It is believed that this is a more realistic value for the accuracy of measurements of the damping moment.

Uncertainties in the density and velocity of the air stream were determined from the least readings of the instruments measuring the tunnel stagnation temperature and pressure. These were ±2° Fahrenheit for the stagnation temperature and ±0.2 centimeter for the mercury manometer measuring stagnation pressure, which led to uncertainties of ±0.2 percent and ±0.9 percent for the density and velocity, respectively.

It was possible to read the time scale on the oscillograph record to ±0.001 second. At 50 cycles per second, this would produce an error in frequency of ±0.4 percent.

The total uncertainty in the damping-moment coefficient was taken to be the square root of the sum of the squares of the effects of the uncertainties mentioned above. This calculation resulted in a total uncertainty of ±0.04.

Examination of the data shows that an uncertainty in the damping-moment coefficient of ±0.04 is unrealistic. During the experiment, a certain amount of free-stream buffeting was present. When it is considered that the damping moments measured were very small, it is quite possible that this buffeting could contribute an appreciable amount of uncertainty to the damping-moment coefficient. Accordingly, the standard deviation of the damping-moment coefficient was calculated for each test point. These results are tabulated in table I.

RESULTS AND DISCUSSION

Theory

At the present time, only one theoretical study of control-surface dynamic stability at supersonic speeds has come to the attention of the author (ref. 6). This paper was concerned with a two-dimensional wing-control-surface combination and was useful in the present case in showing only the trends of the damping with Mach number.

If the usual assumption of small perturbations is made, and if the wing ahead of the control surface is at zero angle of attack, then the control surface can be considered as a separate wing oscillating in the supersonic air stream. Theoretical damping moments were calculated by applying the results of reference 7 which give the forces and moments on harmonically oscillating rectangular wings. While the plan form of the control surface tested was trapezoidal rather than rectangular, it was felt that the effect of the raked tip would be small, particularly at the higher supersonic speeds.

It should also be noted that the results of reference 7 are developed only to the first order in frequency. There are papers on rectangular

wings which present results including the effects of frequency cubed but these results show that for the frequencies of the present investigation the first-order theory is sufficient.

A theoretical solution for subsonic compressible flow exists only for the two-dimensional problem and, then, the results have been tabulated only for Mach numbers up to 0.7. For these reasons, no comparison has been made with theory for the subsonic results.

Damping Moments

The results of the tests of the torsional damping characteristics of the control surface are shown in figures 7, 8, and 9. The results are presented as the variation of the nondimensional damping parameter, $C_{h_{\dot{\delta}}}$, with Mach number for the various conditions tested.

Effect of control-surface oscillation amplitude.- A plot of $C_{h_{\dot{\delta}}}$ versus Mach number at zero angle of attack for the three oscillation amplitudes tested is shown in figure 7. The general trend of the damping coefficients with supersonic Mach number is from slightly unstable damping at a Mach number of 1.3 to neutral stability at the higher Mach numbers. The data are quite consistent in indicating this trend. There is, however, a significant difference between experiment and theory at the higher Mach numbers. At the present time, no reasonable explanation has been advanced to explain the discrepancy. It should be noted here again that the theoretical results shown were calculated for a rectangular plan form; whereas the control surface tested had a trapezoidal plan form. This fact, however, cannot explain the lack of agreement at the higher Mach numbers where the tip effect becomes negligible.

The data at subsonic speeds show stable damping over the Mach number range tested.

It can be seen that the results for oscillation amplitudes of the flap, δ_o, of 5° and 3° are essentially the same for the supersonic Mach numbers. It is difficult to evaluate the results at $\delta_o = 1^\circ$ since, as is shown in table I, those data show a considerably larger standard deviation than the remainder of the data.

The oscillation amplitude had little effect on the damping at subsonic speeds except at a Mach number of 0.9, and the results obtained at this Mach number are in question because of possible wind-tunnel-wall effects.

Effect of angle of attack.- Figure 8 shows the variation of $C_{h_{\dot{\delta}}}$ with Mach number for several angles of attack at each oscillation

amplitude. The effect of a variation in angle of attack on C_{h_δ} appears to be within the standard deviation of the data as shown in table I, except for the results obtained at supersonic speeds at an oscillation amplitude of 3°. For those data, an increase in angle of attack had a small but consistent stabilizing effect throughout the Mach number range.

Effect of frequency.- Data were obtained for all test points at approximately 25 and 50 cycles per second, which correspond to reduced frequencies, k, of 0.015 and 0.030, respectively, at a Mach number of 1.3. At supersonic speeds, no consistent effect of frequency was noted. Reference 8 shows that, for these reduced frequencies, no effect is to be expected.

The data obtained at subsonic speeds show an increase in the damping-moment coefficient with an increase in frequency which is consistent with the trends shown in the two-dimensional analysis presented in reference 9. These data must be interpreted, however, in the light of the possible effect of the tunnel walls, as pointed out in the section Corrections to Data.

Effect of boundary-layer transition.- The results of the tests with boundary-layer transition fixed are shown in figure 9. The data show that the effect of fixing the transition of the boundary layer was small for both the 5° and 1° control-surface amplitude.

Restoring Moments

The results of the determination of the in-phase aerodynamic moments acting on the control surface are presented in figure 10. Comparison is made with data obtained on a static test model which was geometrically similar to the model used in this investigation. The close agreement of the static and dynamic data confirms the results obtained from theory, which show that for the reduced frequencies of this test, the effects of frequency on the restoring moments are negligible.

CONCLUSIONS

The results of the investigation of the torsional damping characteristics of a constant-chord control surface mounted on an aspect ratio 2 triangular wing produced the following conclusions:

1. The cancellation technique provided a means of circumventing the difficulties associated with the measurement of the total aerodynamic moment and phase angle and permitted a simple, accurate determination of the aerodynamic damping in forced-oscillation tests.

2. The torsional damping of the control surface at supersonic speeds varied from a small degree of instability at a Mach number of 1.3 to neutral stability at a Mach number of 1.9. The magnitude of the damping moment cannot be accurately predicted by the theories used in this report.

3. The damping coefficient of the control surface at subsonic speeds was stable throughout the Mach number range.

4. There was little effect of control-surface oscillation amplitude on the damping coefficient.

5. The effect of angle of attack on the damping coefficient was within the standard deviation of the data for all conditions except in the supersonic Mach number range at an oscillation amplitude of 3°. For these conditions, an increase in angle of attack had a stabilizing effect.

6. The damping coefficient was essentially constant with variations in frequency up to the maximum reduced frequency of the investigation, 0.030, for supersonic Mach numbers. At subsonic speeds, the damping coefficient increased with increasing frequency, following the trends shown by two-dimensional theory. However, the wind-tunnel walls might have had some effect on the damping coefficient at subsonic speeds.

7. The aerodynamic restoring moments measured at 50 cycles per second were in reasonable agreement with those obtained in static tests.

Ames Aeronautical Laboratory
National Advisory Committee for Aeronautics
Moffett Field, Calif.

REFERENCES

1. Frick, Charles W., and Olson, Robert N.: Flow Studies in the Asymmetric Adjustable Nozzle of the Ames 6- by 6-foot Supersonic Wind Tunnel. NACA RM A9E24, 1949.

2. Gonzoule, Thomas, Smith, Rodney H., and Porter, Robert G.: The Design and Construction of an Airfoil Oscillator (Phase 2 and Phase 3). Mass Inst. of Tech. Flutter Research Laboratory. Oct. 15, 1945.

3. Runyan, Harry L., and Watkins, Charles E.: Considerations on the Effect of Wind-Tunnel Walls on Oscillating Air Forces for Two-Dimensional Subsonic Compressible Flow. NACA TN 2552, 1952.

[redacted]

[redacted]

4. Runyan, Harry L., Woolston, Donald S., and Rainey, A. Gerald: A Theoretical and Experimental Study of Wind-Tunnel Effects on Oscillating Air Forces for Two-Dimensional Subsonic Compressible Flow. NACA RM L52I17a, 1953.

5. Herriot, John G.: Blockage Corrections for Three-Dimensional-Flow Closed-Throat Wind Tunnels with Consideration of the Effect of Compressibility. NACA Rep. 995, 1950. (Supersedes NACA RM A7B28)

6. Huckel, Vera, and Durling, Barbara J.: Tables of Wing-Aileron Coefficients of Oscillating Air Forces for Two-Dimensional Supersonic Flow. NACA TN 2055, 1950.

7. Watkins, Charles E.: Effect of Aspect Ratio on Undamped Torsional Oscillations of a Thin Rectangular Wing in Supersonic Flow. NACA TN 1895, 1949.

8. Watkins, Charles E.: Effect of Aspect Ratio on the Air Forces and Moments of Harmonically Oscillating Thin Rectangular Wings in Supersonic Potential Flow. NACA TN 2064, 1950.

9. Tobak, Murray: Damping in Pitch of Low-Aspect-Ratio Wings at Subsonic and Supersonic Speeds. NACA RM A52L04a, 1953.

TABLE I.- STANDARD DEVIATIONS OF TEST DATA

M	$\delta_o = 1^\circ$		$\delta_o = 3^\circ$		$\delta_o = 5^\circ$	
	$\alpha = 0^\circ$					
	f = 25	f = 50	f = 25	f = 50	f = 25	f = 50
1.9	0.482	0.463	0.015	0.090	0.095	0.087
1.6	.434	.591	.115	.144	.042	.057
1.3	.694	.061	.021	.046	.007	.028
.9	.085	.409	.162	.284	.471	.157
.8	.520	.326	.111	.125	.288	.007
.6	.153	.851	.115	.191	.093	.000
$\alpha = 5^\circ$						
.9	0.850	0.481	0.102	0.399	- - -	- - -
.8	.238	.255	.217	.130	- - -	- - -
.6	.367	.294	.064	.061	- - -	- - -
$\alpha = 10^\circ$						
1.9	0.055	0.171	0.210	0.060	0.135	0.068
1.6	.440	.358	.042	.130	.150	.075
1.3	.765	.206	.095	.144	.137	.111

[redacted]

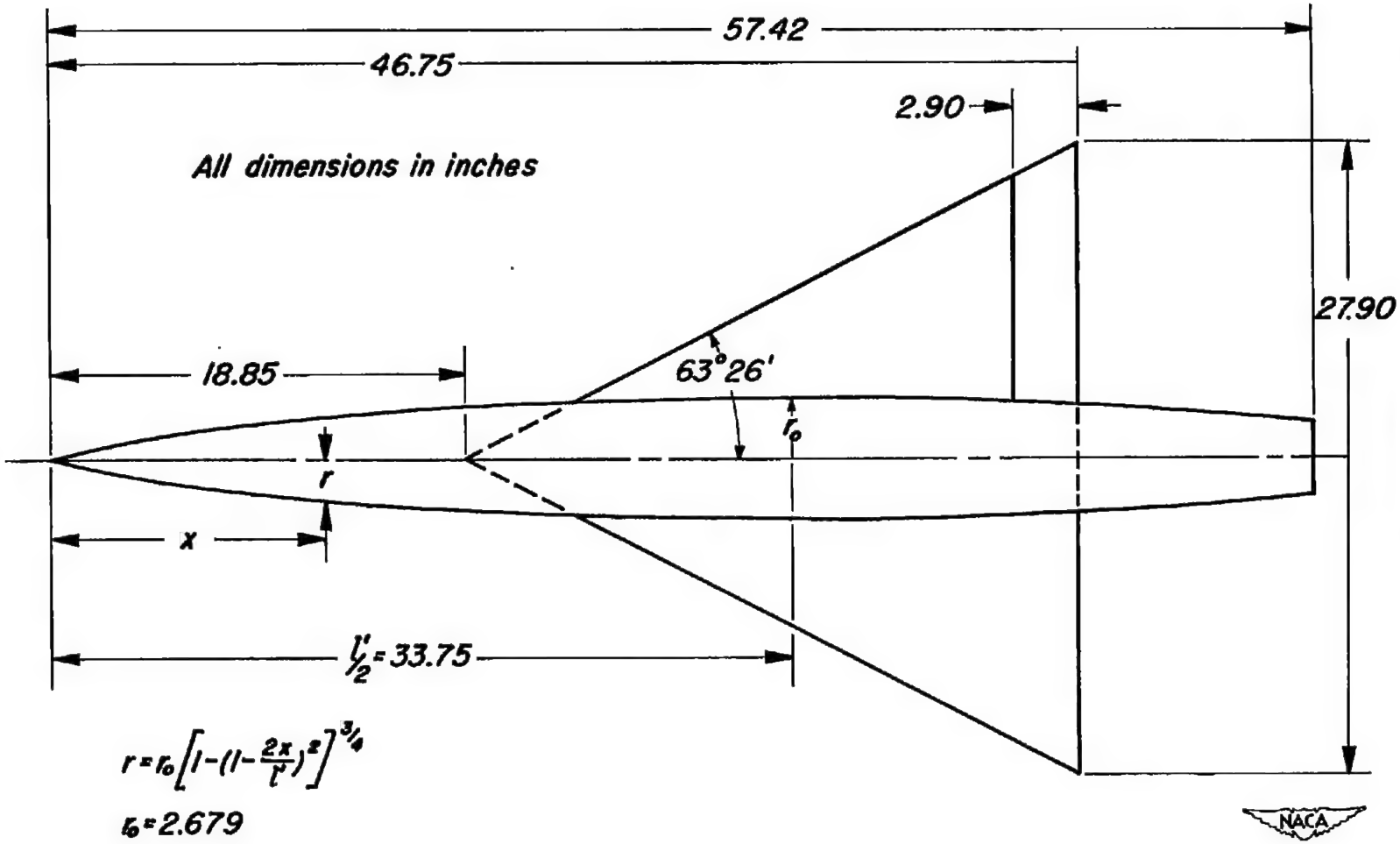

Figure 1.— Sketch of model.

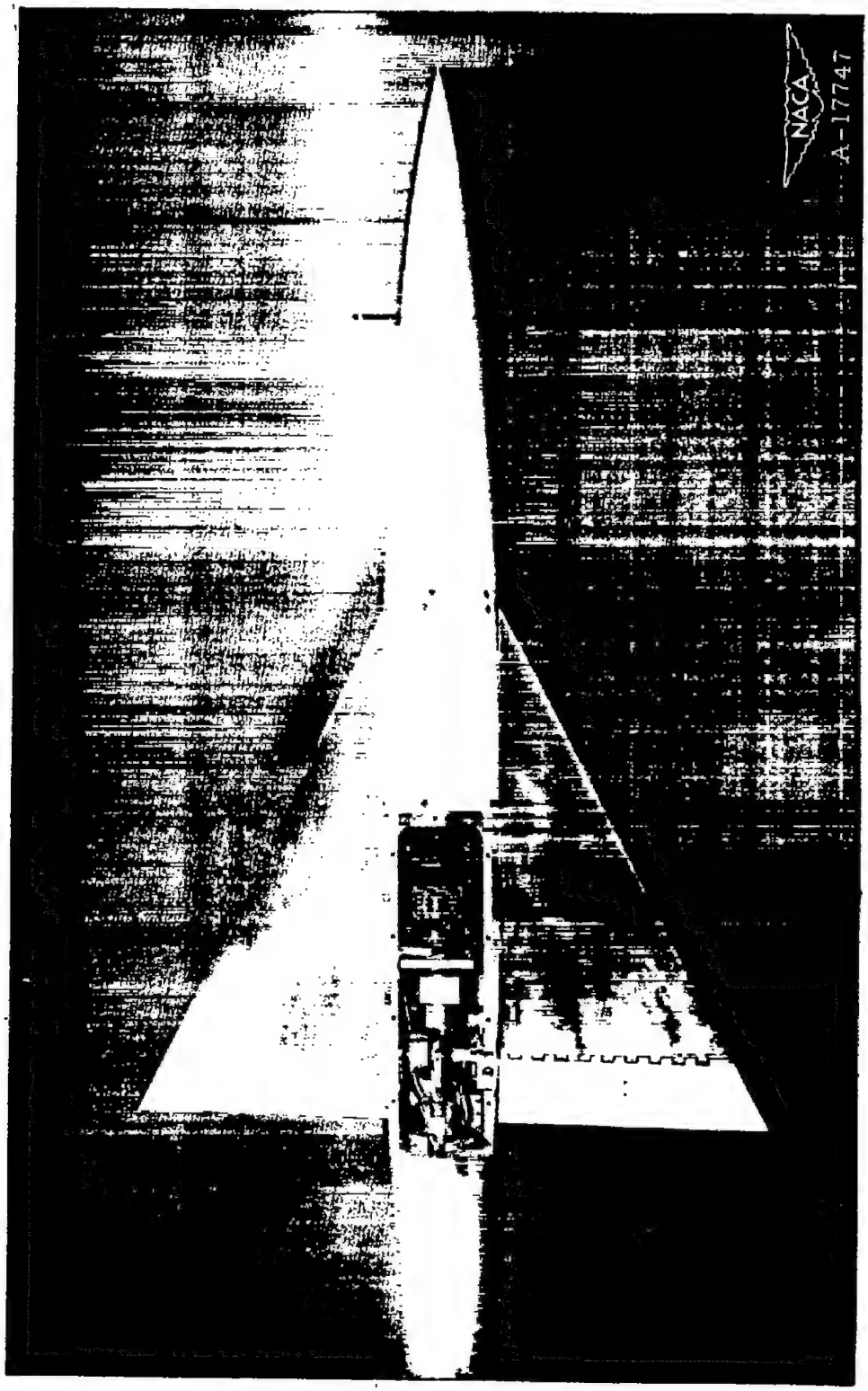

Figure 2.- Photograph of model.

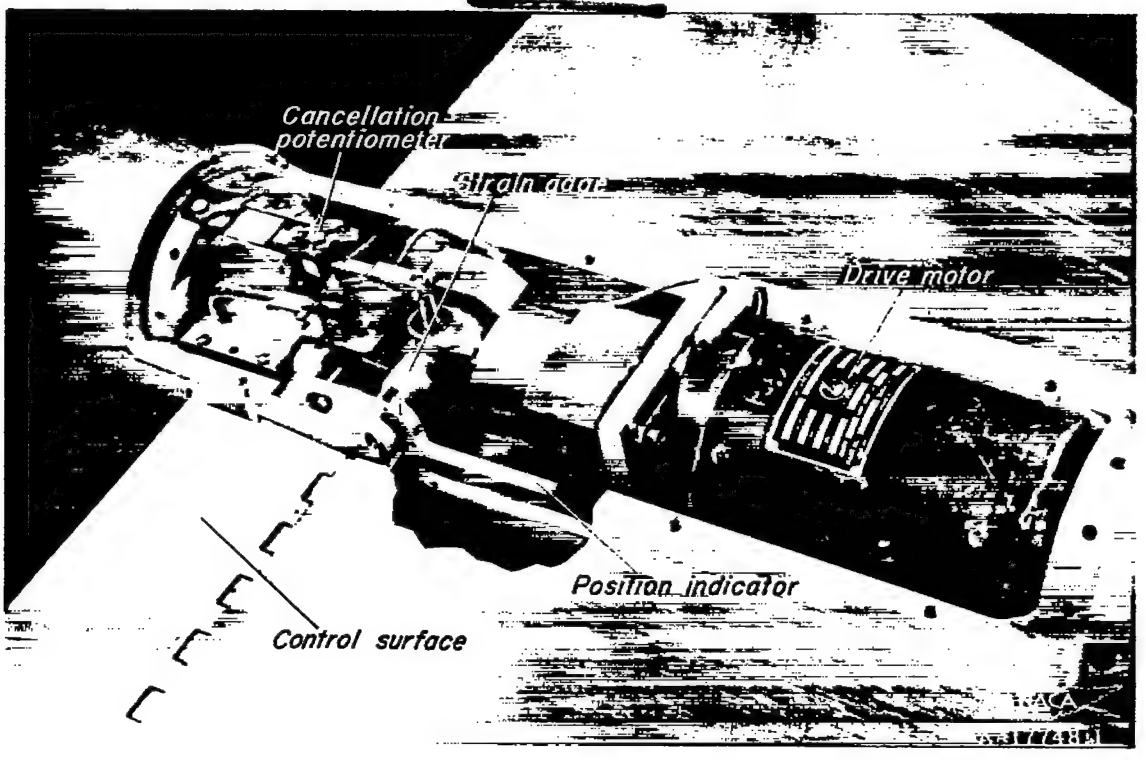

(a) Three-quarter front view.

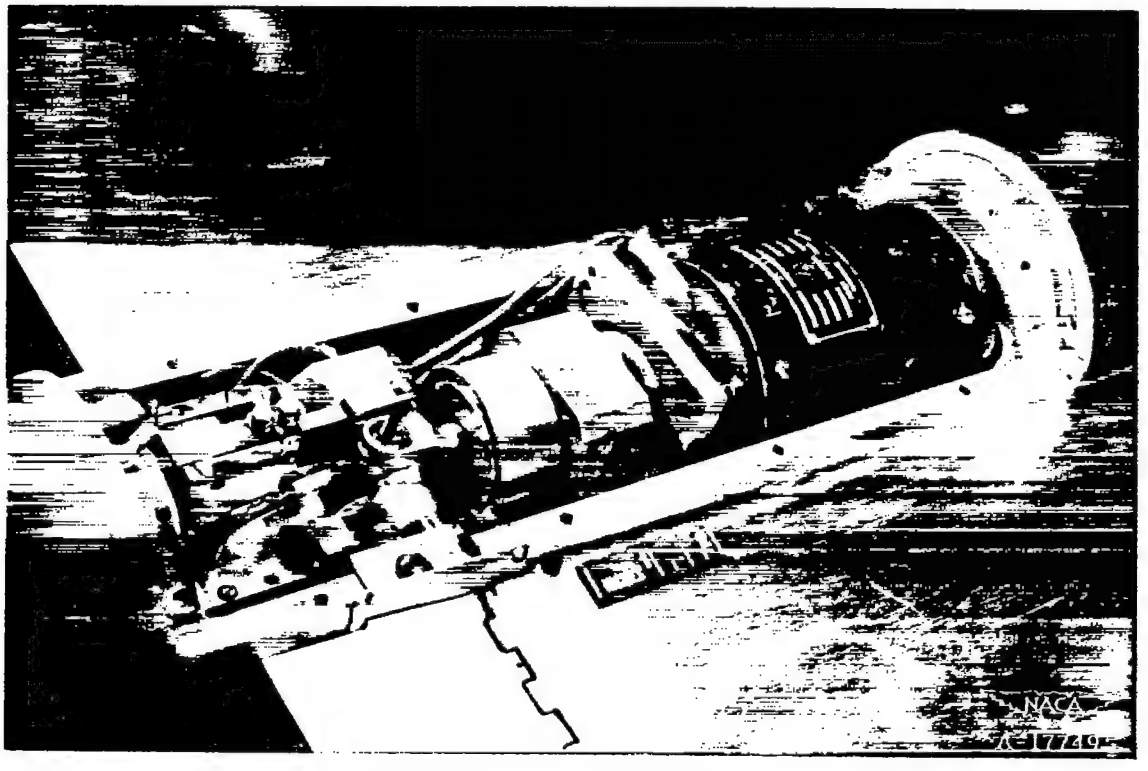

(b) Three-quarter rear view.

Figure 3.- Photographs of drive mechanism.

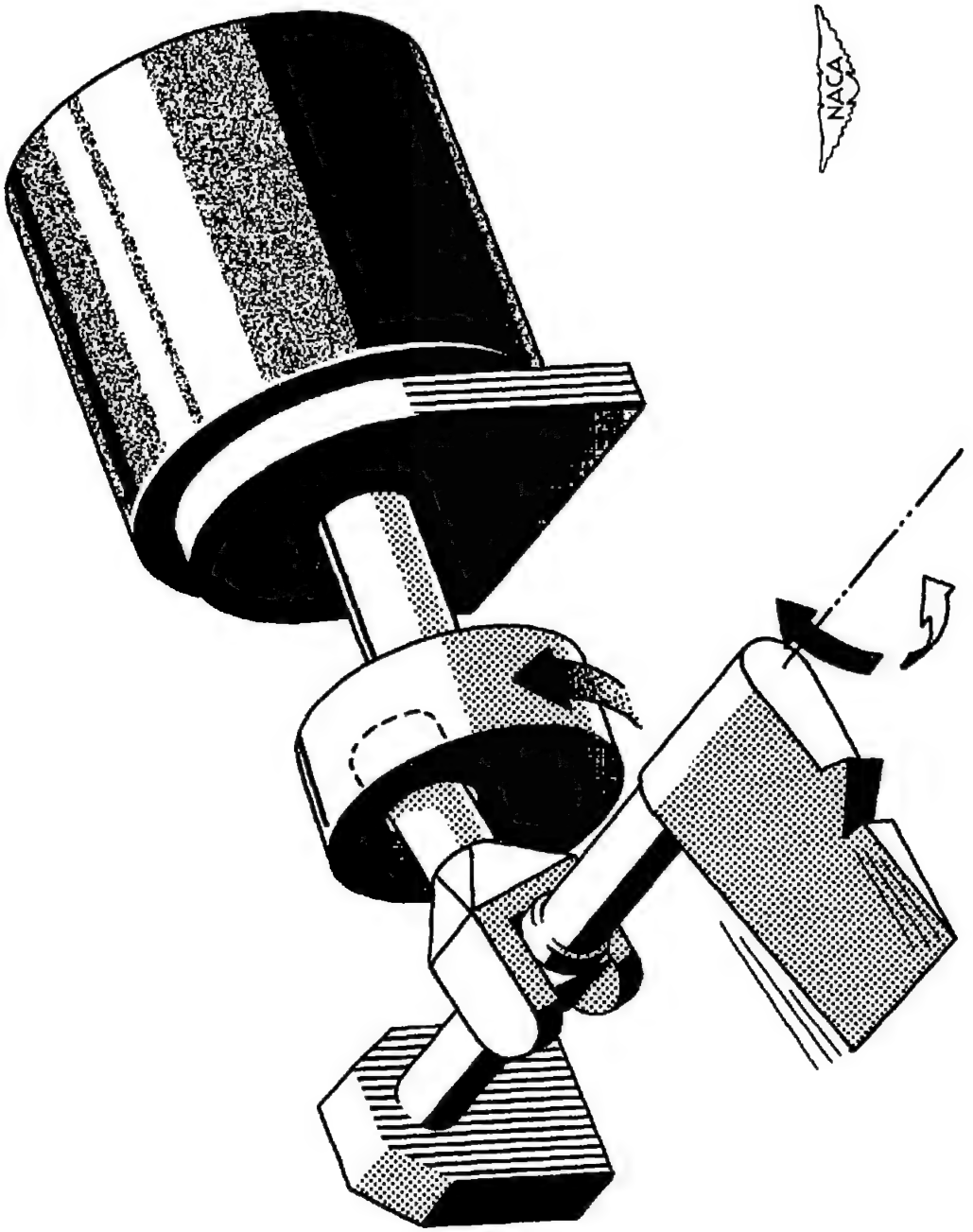

Figure 4.- Schematic drawing of drive linkage.

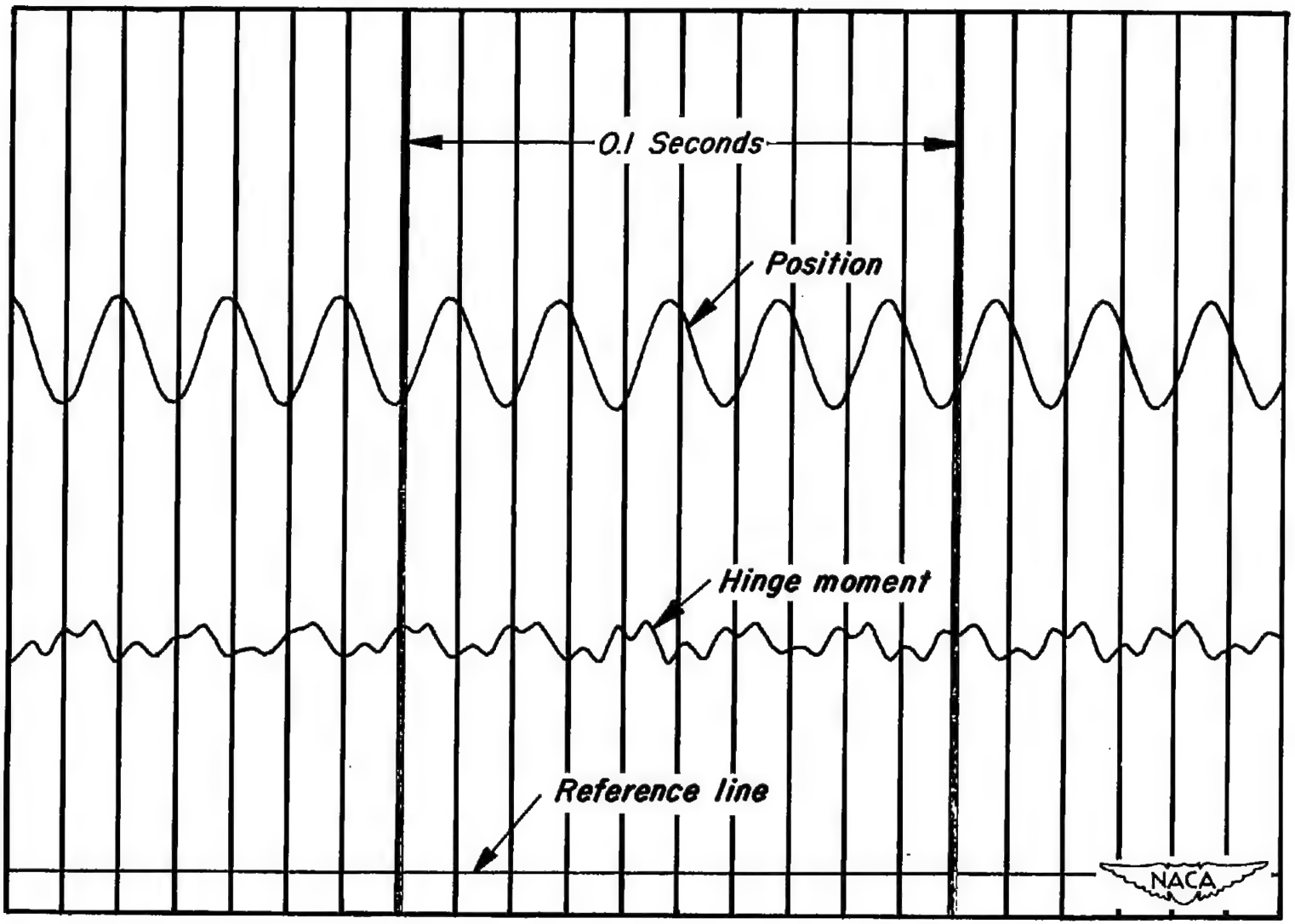

Figure 5. Typical oscillograph record.

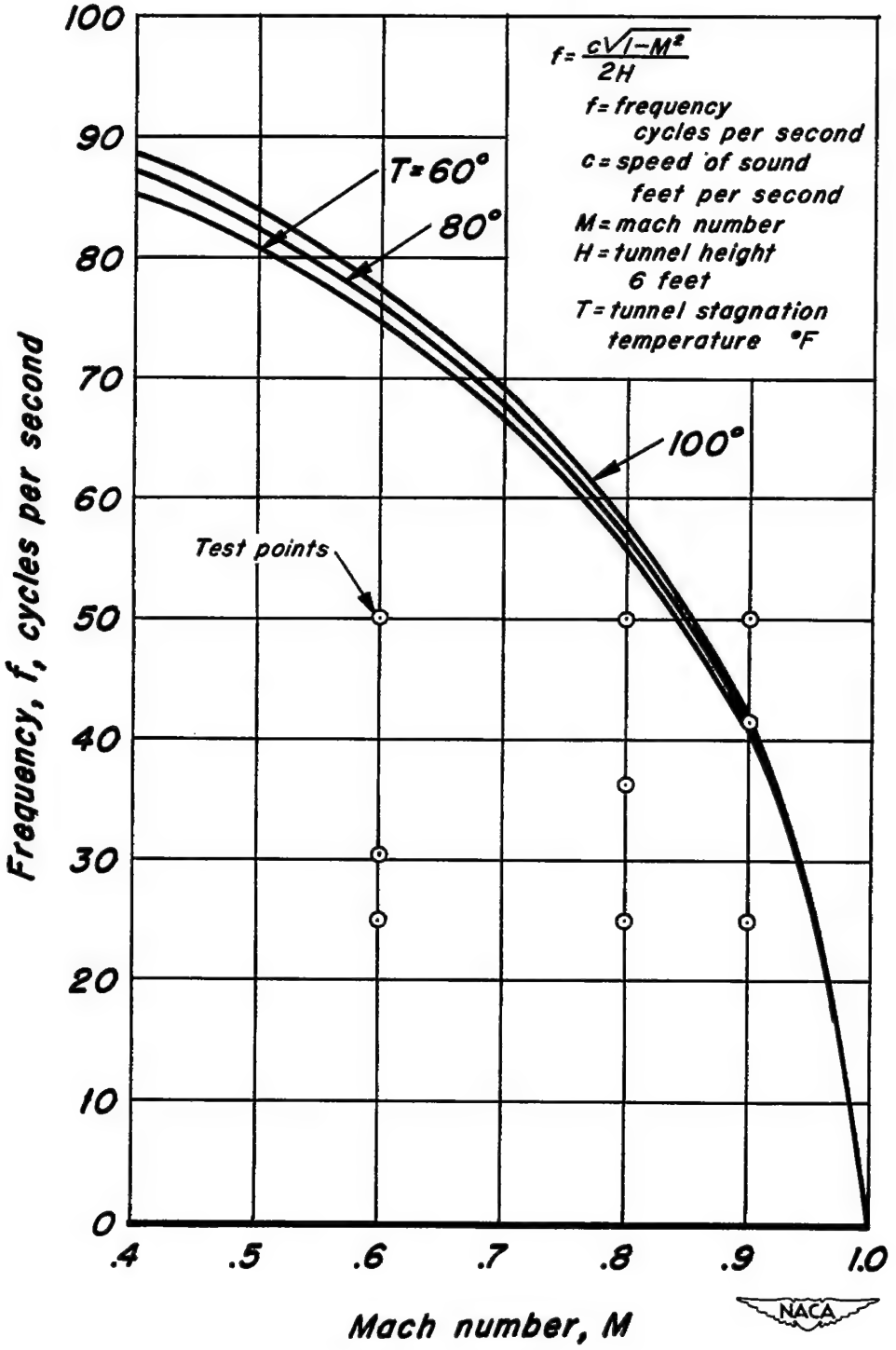

Figure 6.- Theoretical wind-tunnel resonant frequency.

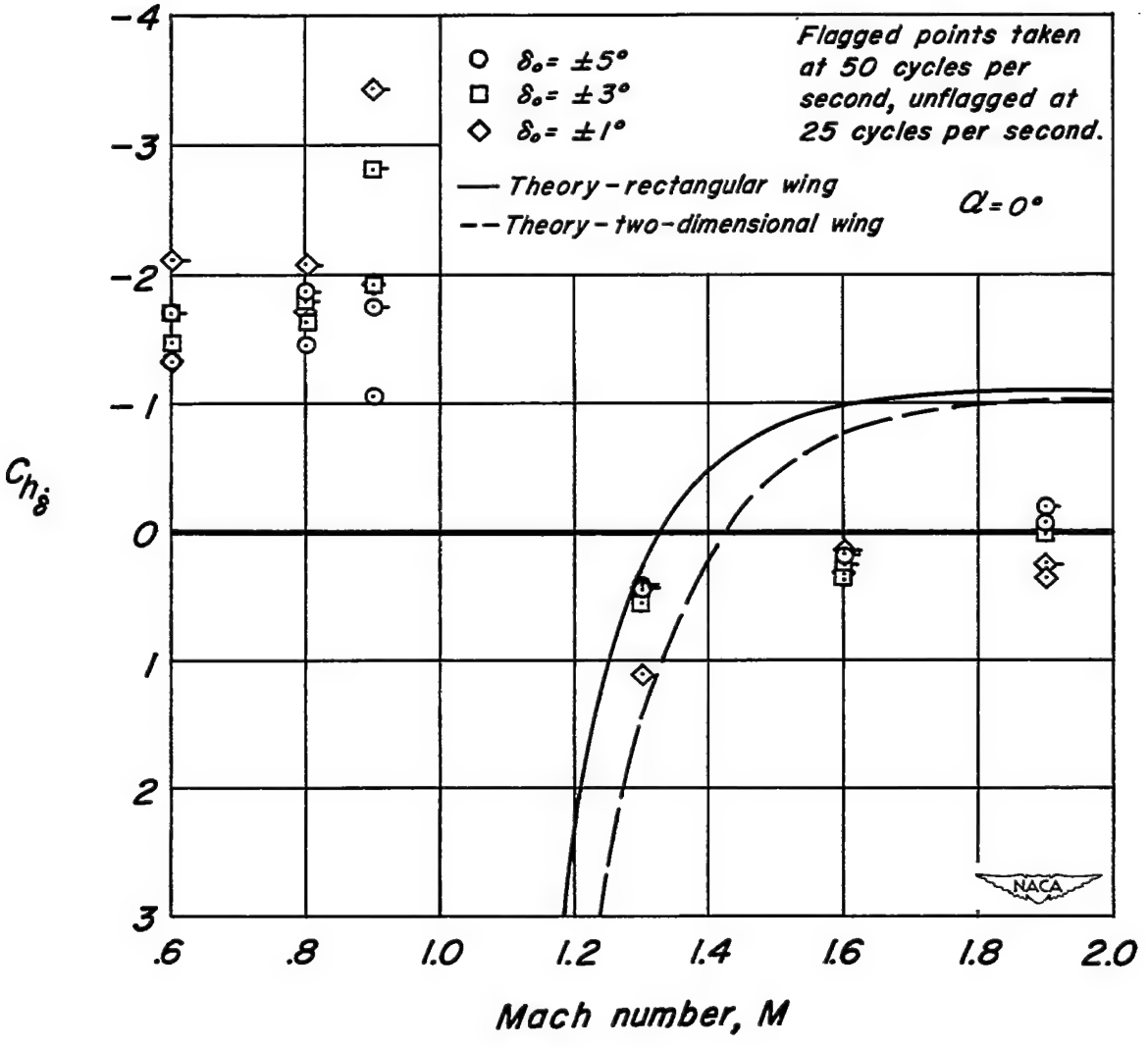

Figure 7.– The variation of damping coefficient with Mach number for three values of control-surface oscillation amplitude.

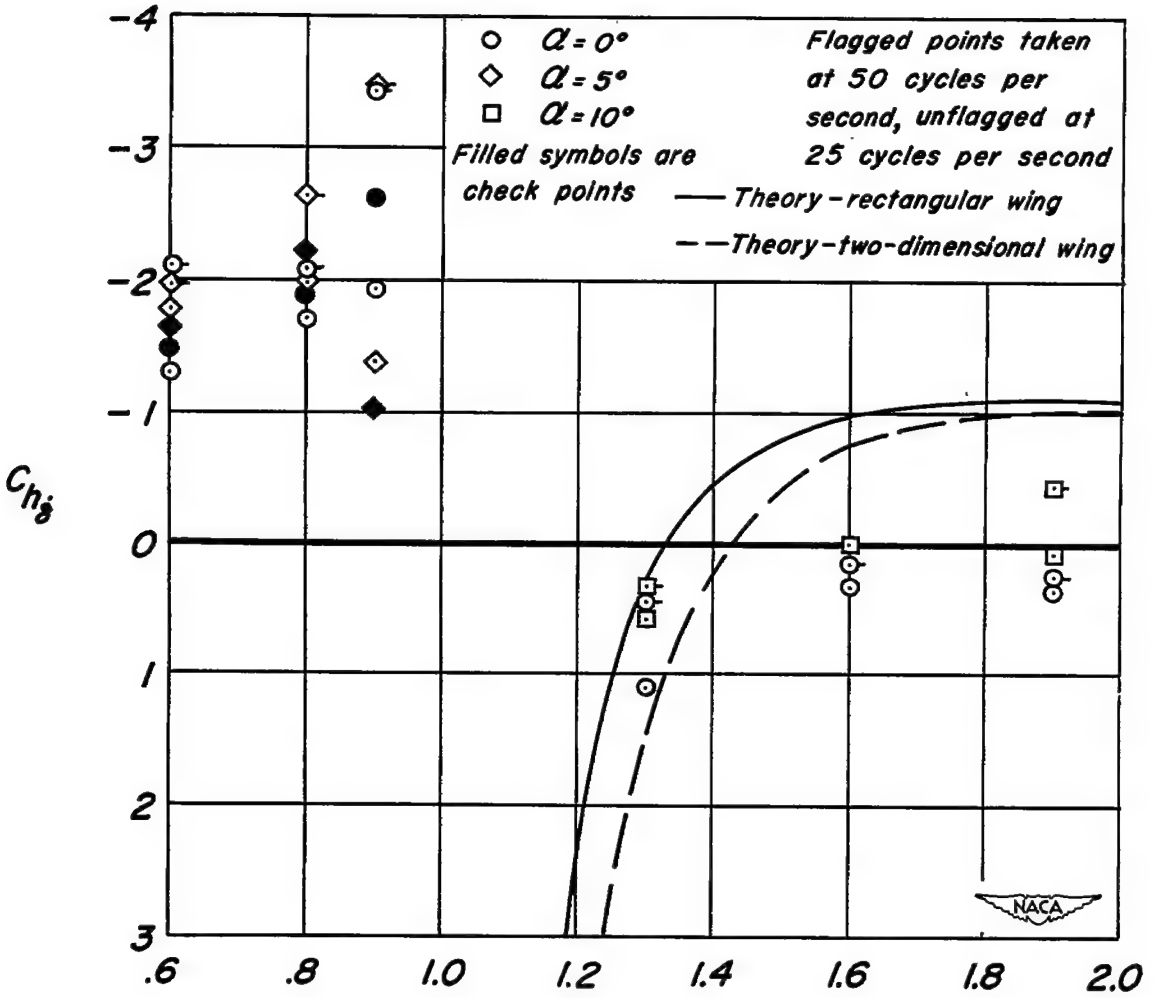

(a) $\delta_o = \pm 1°$

Figure 8.— The variation of damping coefficient with Mach number for three angles of attack.

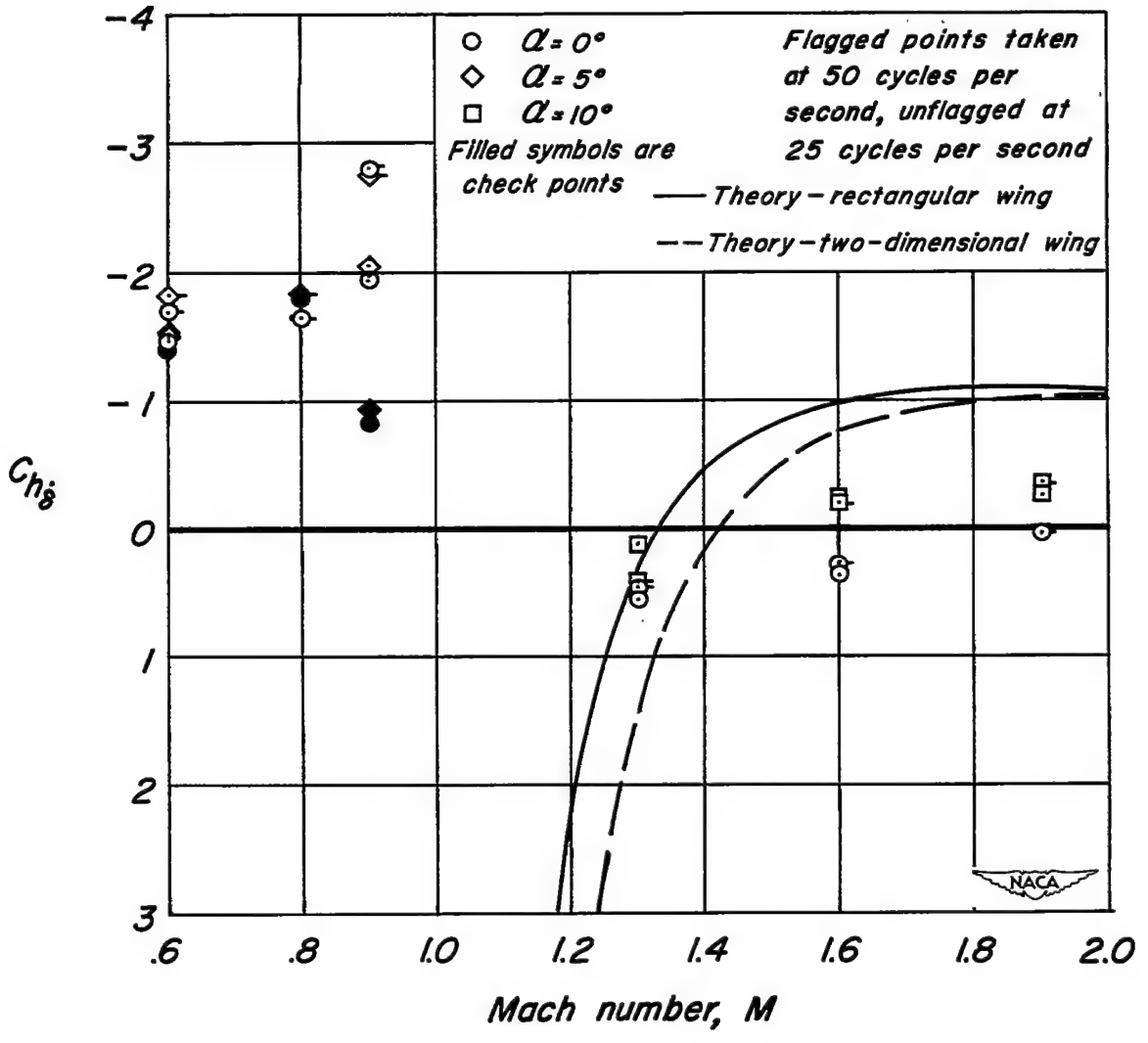

(b) $\delta_o = \pm 3°$

Figure 8.– Continued.

[redacted]

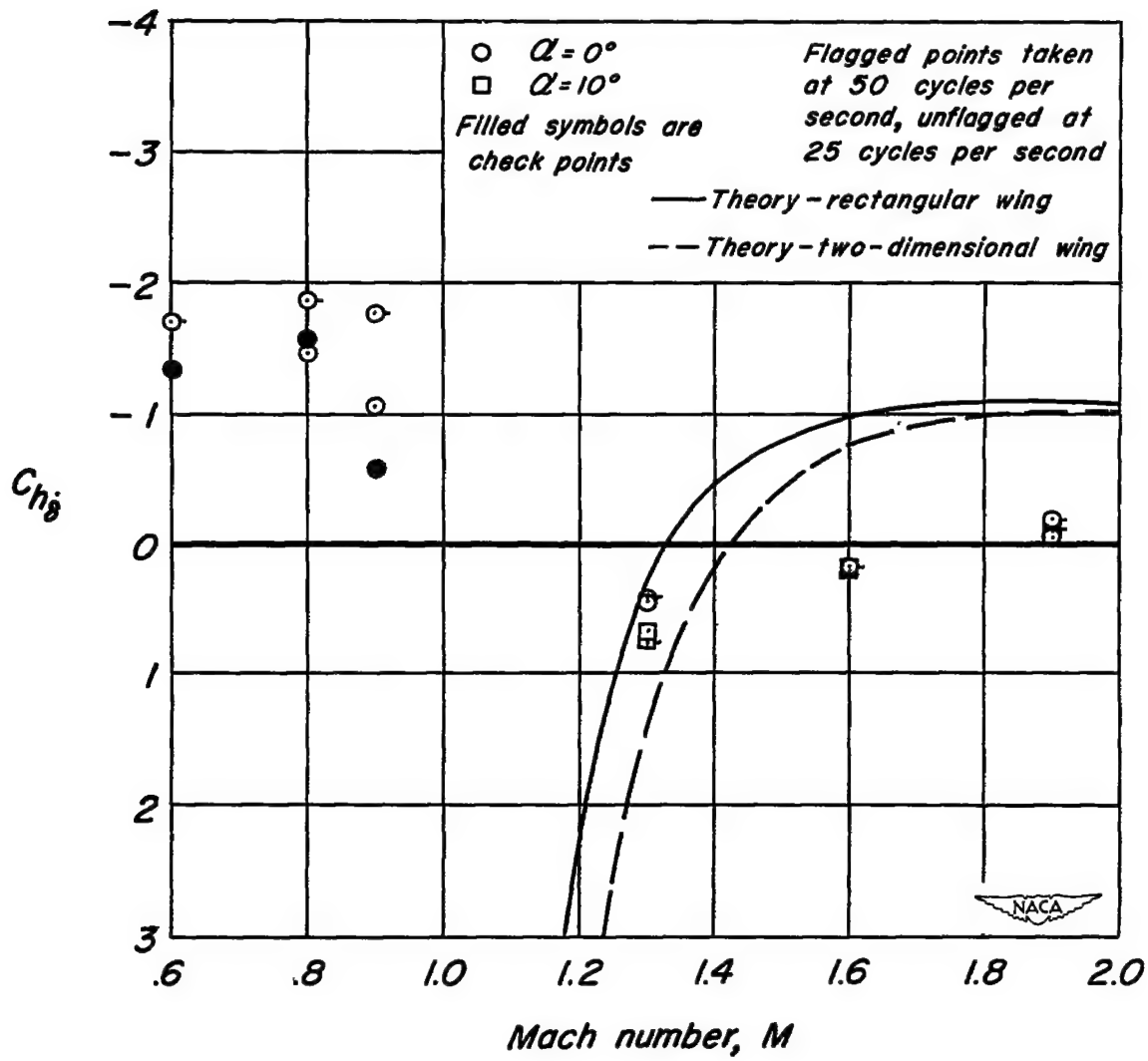

(c) $\delta_o = \pm 5°$

Figure 8.– Concluded.

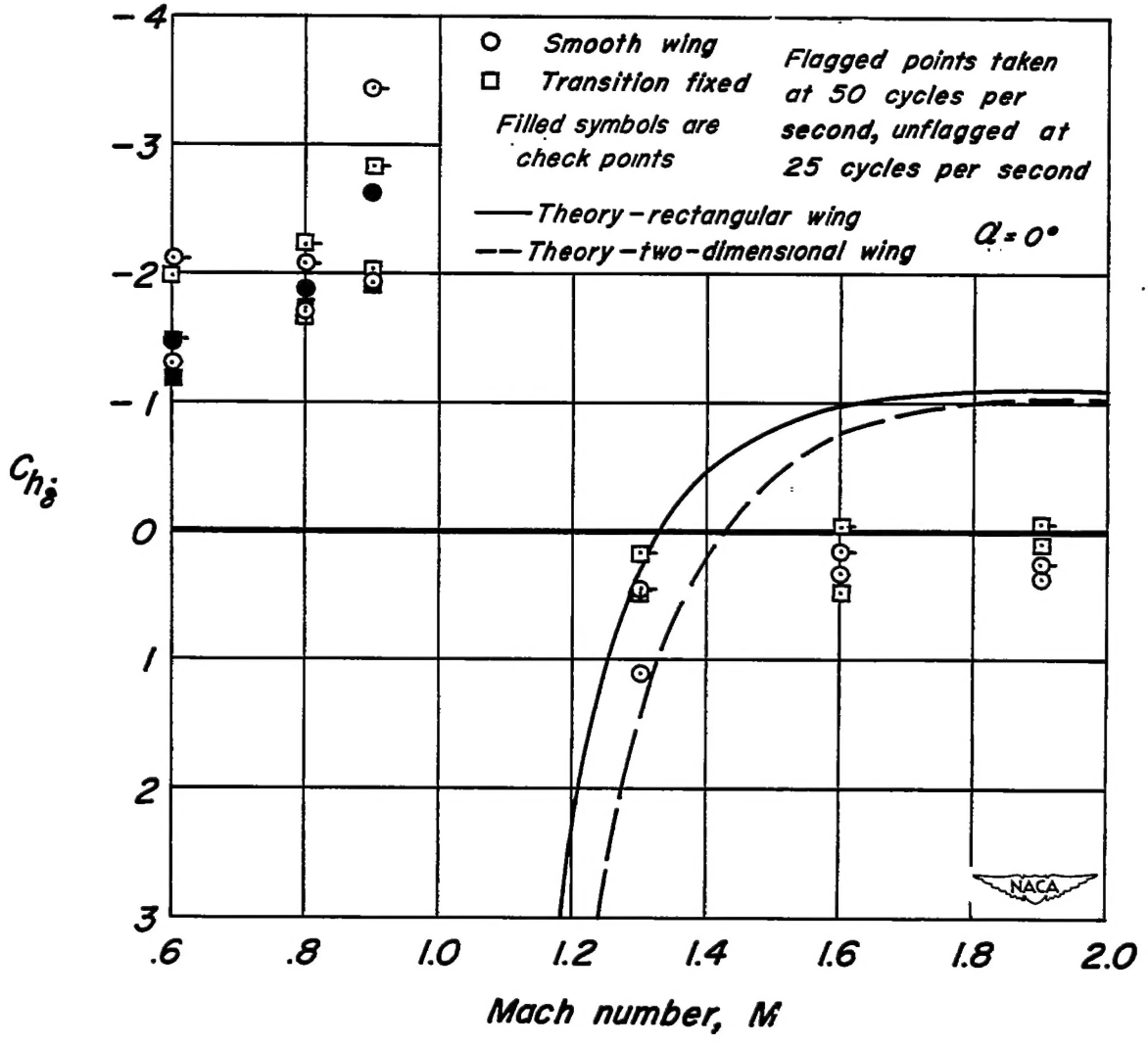

(a) $\delta_o = \pm 1°$

Figure 9.– The effect of boundary-layer transition on the damping-moment coefficient, $C_{h_\dot{\delta}}$.

[redacted]

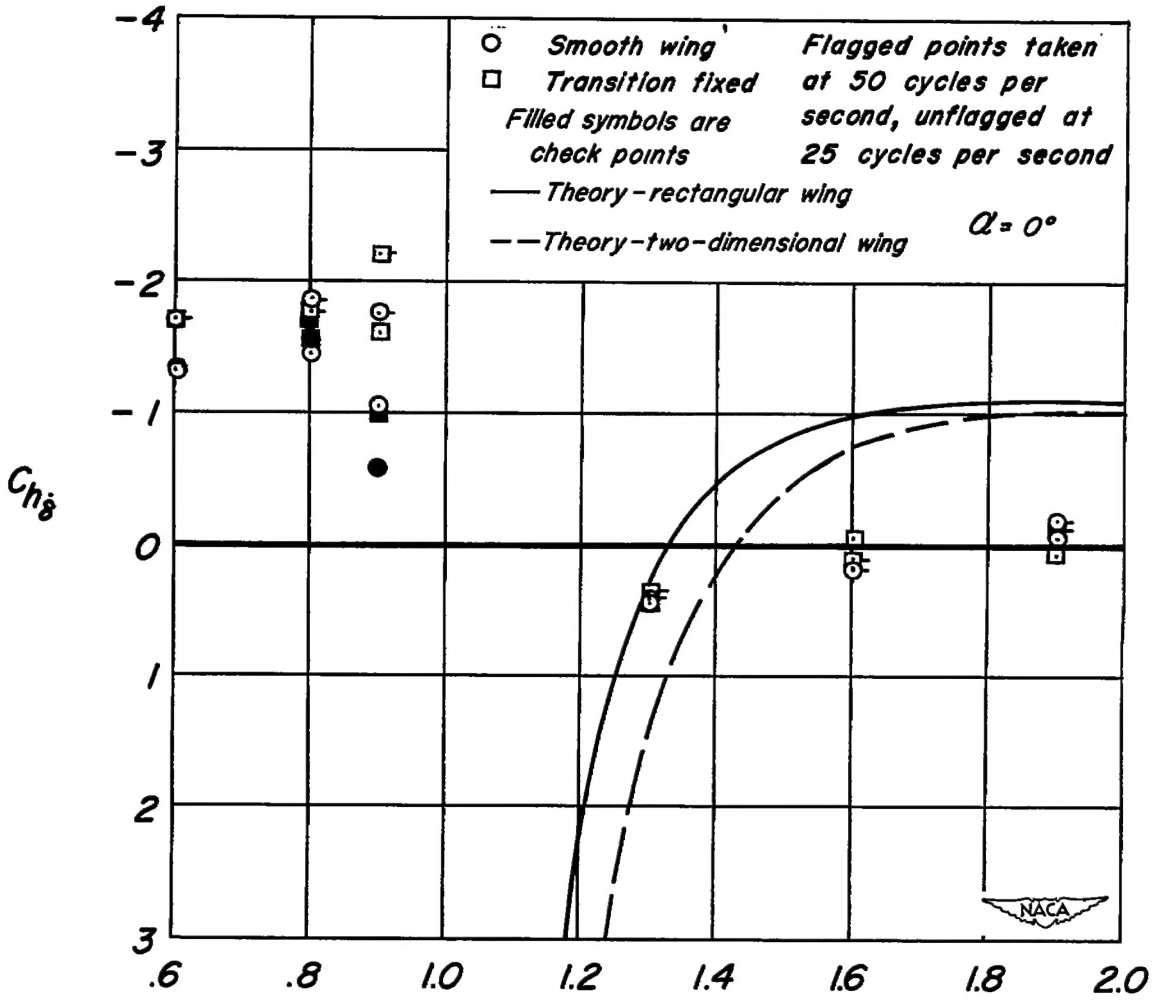

(b) $\delta_o = \pm 5°$

Figure 9.- Concluded.

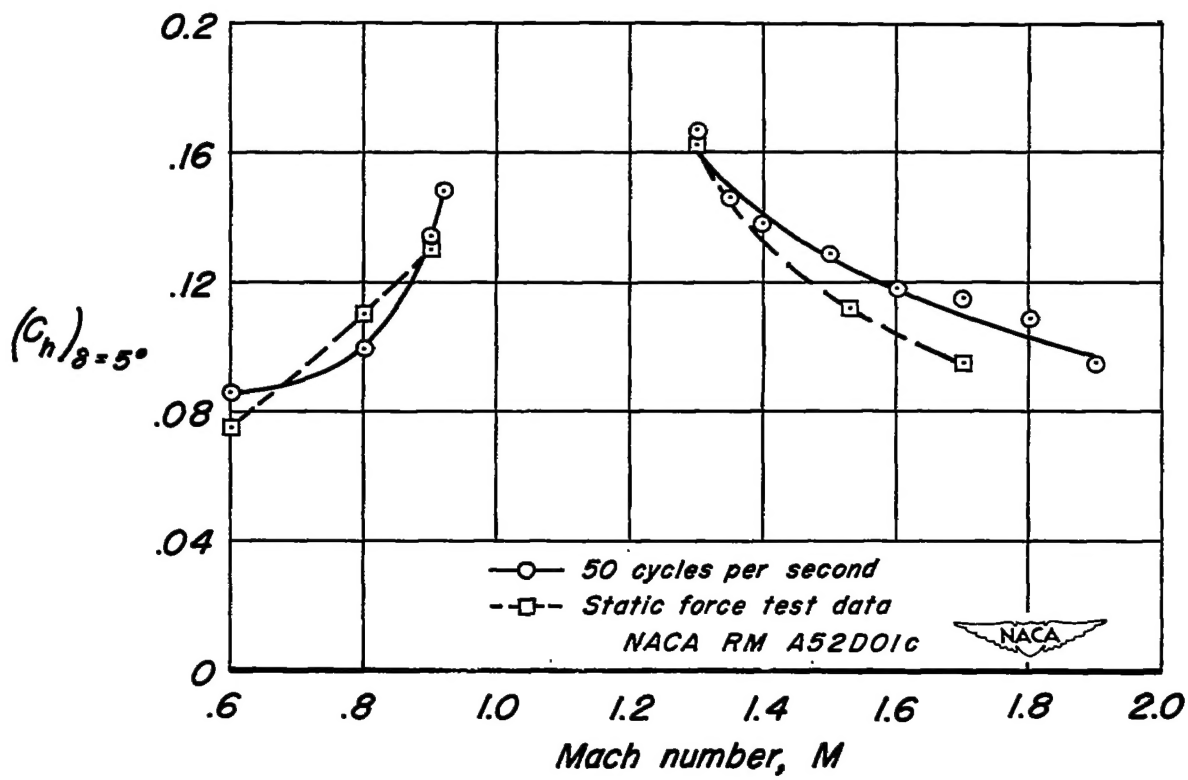

(a) $\alpha = 0°$

Figure 10.– The variation of aerodynamic restoring–moment coefficient with Mach number.

[redacted]

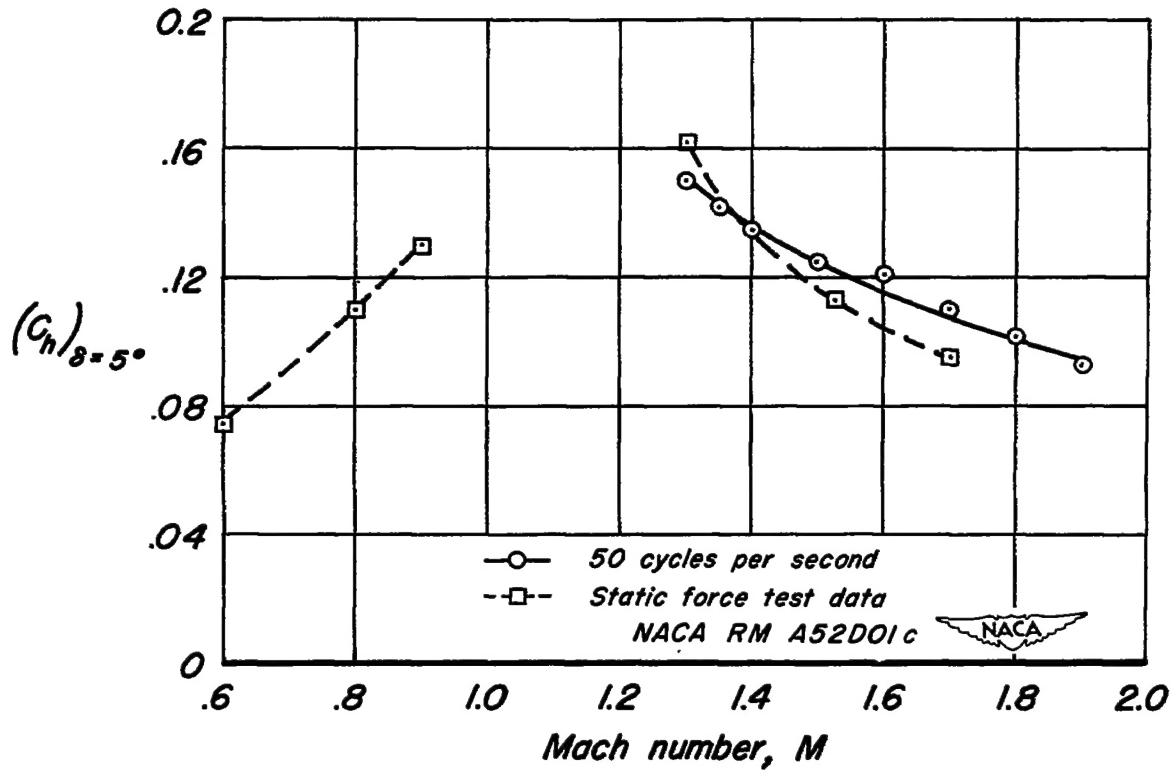

(b) $\alpha = 5°$

Figure 10.– Concluded.

NACA-Langley - 7-2-53 - 400